REGULAR ARTICLE

blood advances

CXCR5 and ICOS expression identifies a CD8 T-cell subset with T_{FH} features in Hodgkin lymphomas

Kieu-Suong Le,[1,2] Patricia Amé-Thomas,[3,4] Karin Tarte,[3,4] Françoise Gondois-Rey,[1] Samuel Granjeaud,[1] Florence Orlanducci,[5] Etienne D. Foucher,[1] Florence Broussais,[5] Reda Bouabdallah,[5] Thierry Fest,[3,4] Dominique Leroux,[6] Sapna Yadavilli,[7] Patrick A. Mayes,[7] Luc Xerri,[1,2,5,*] and Daniel Olive[1,2,5,*]

[1]Centre de Recherche en Cancérologie de Marseille, Centre National de la Recherche Scientifique U7258/INSERM U1068, Marseille, France; [2]Faculté de Médecine, Aix Marseille Université, Marseille, France; [3]LabEx IGO, Equipe Labellisée Ligue Contre le Cancer, Etablissement Français du Sang Bretagne, Université de Rennes 1, Unité Mixte de Recherche U1236, INSERM, Rennes, France; [4]Pôle Biologie, Centre Hospitalier Universitaire de Rennes, Rennes, France; [5]Institut Paoli-Calmettes, Marseille, France; [6]Institut Albert Bonniot, Grenoble, France; and [7]Immuno-Oncology and Combination Discovery Performance Unit, Oncology Research and Development, GlaxoSmithKline, Collegeville, PA

Key Points

- A subset of CD8 T cells in some Hodgkin lymphomas shares phenotypic and functional features with CD4 T_{FH} cells.

A better characterization of T-cell subsets in the microenvironment of classical Hodgkin lymphoma (cHL) would help to develop immunotherapies. Using multicolor flow cytometry, we identified in 6 of 43 cHL tissue samples a previously unrecognized subset of CD8 T cells coexpressing CXCR5 and inducible T-cell costimulator (ICOS) molecules ($CD8_{CXCR5+ICOS+}$). These cells shared phenotypic features with follicular helper T (T_{FH}) cells including low CCR7 expression together with high expression of B-cell lymphoma-6, programmed cell death 1, B and T lymphocyte attenuator, CD200, and OX40. They had deficient cytotoxicity, low interferon-γ secretion, and common functional properties with intratumoral $CD4^+$ T_{FH} cells, such as production of interleukin-4 (IL-4), IL-21, CXCL13, and capacity to sustain B cells. Gene profiling analysis showed a significant similarity between the signatures of $CD8_{CXCR5+ICOS+}$ T cells and $CD4^+$ T_{FH} cells. Benign lymphadenitis tissues (n = 8) were devoid of $CD8_{CXCR5+ICOS+}$ cells. Among the 35 B-cell lymphoma tissues analyzed, including follicular lymphomas (n = 13), diffuse large cell lymphomas (n = 12), marginal zone lymphomas (MZLs; n = 3), mantle cell lymphomas (n = 3), and chronic lymphocytic leukemias (n = 4), only 1 MZL sample contained $CD8_{CXCR5+ICOS+}$ cells. Lymphoma tumors with $CD8_{CXCR5+ICOS+}$ cells shared common histopathological features including residual germinal centers, and contained high amounts of activated $CD8_{CXCR5-ICOS+}$ cells. These data demonstrate a CD8 T-cell differentiation pathway leading to the acquisition of some T_{FH} similarities. They suggest a particular immunoediting process with global CD8 activation acting mainly, but not exclusively, in HL tumors.

Introduction

The tumor microenvironment is known to play a role in lymphoma pathogenesis.[1] Classical Hodgkin lymphoma (cHL) tissues contain a considerable proportion of reactive immune cells when compared with the paucity of neoplastic Reed-Sternberg (RS) cells.[2] Using gene expression analyses, we and others have shown that the amount of reactive B cells and macrophages influences the outcome of cHL

Submitted 10 February 2018; accepted 15 June 2018. DOI 10.1182/bloodadvances.2018017244.

*L.X. and D.O. contributed equally to this work.

The microarray data reported in this article have been deposited in the Gene Expression Omnibus database (accession numbers GSE74982 [for T_{FH} and memory CD4 T cells of tonsil] and GSE74983 [for $CD8_{CXCR5+ ICOS+}$ and $CD8_{CXCR5-ICOS-}$ from cHL]).

The full-text version of this article contains a data supplement.

patients.[3-6] Although a specific gene signature evocative of an antiviral response was reported in Epstein-Barr virus–positive (EBV$^+$) cHL tumors,[5] there is to date only scant evidence supporting the hypothesis of an intratumoral immune reaction. It has been suggested that a predominant T helper 1 (Th1) reaction may occur in cHL[7] tissues, but a precise characterization of the different T-cell subsets within cHL tumors is still lacking.

Follicular helper T (T_{FH}) cells are CD4 Th cells specialized in supporting humoral immune responses and characterized by high expression of CXCR5 and downregulation of CCR7 in secondary lymphoid organs. They are thus able to migrate into B-cell follicles in response to CXCL13,[8,9] where they provide multiple help signals to B cells.[10] They exhibit a specific phenotypic profile including high expression of CD40L, inducible T-cell costimulator (ICOS), OX40, programmed cell death 1 (PD-1), B and T lymphocyte attenuator (BTLA), CD84/SAP, and B-cell lymphoma-6 (Bcl-6), together with high production of interleukin-21 (IL-21) and CXCL13.[10] Recent studies have shown unexpected heterogeneity and plasticity among T_{FH} cells, due to different T_{FH} subgroups with different phenotypes, functions and anatomical localizations.[11-15] In addition, non-Th cells including regulatory T cells,[16,17] invariant natural killer T (iNKT) cells,[18,19] and γδT cells[20] can be located in B-cell follicles and share phenotypic features with T_{FH} cells, increasing the complexity of T_{FH} cells definition.

CD8 T cells represent 1 of the most important cell type involved in antitumor responses by their capacity of releasing cytolytic molecules and/or by producing effector cytokines like interferon-γ (IFN-γ).[21] Accumulating data have supported the hypothesis of multiple CD8 T-cell subsets with different functions depending on pathological conditions and localizations, as illustrated by the subset of CD8 T cells with suppressive functions identified in inflammatory states,[22] autoimmune disease[23] and cancer.[24-26] To this extent, several recent studies in mice models have highlighted the accumulation of antigen-specific CXCR5$^+$ CD8 T cells in lymphoid tissues during chronic viral infection.[27-29] When compared with regular CD8 T cells, the CXCR5$^+$ subset exhibits a less exhausted phenotype and a unique gene signature related to T_{FH} cells.[27-29] In human, a subset of CD8 T cells expressing CXCR5 has been previously detected in B-cell follicles of normal tonsils,[30] in nasal polyps,[31] in HIV-infected patients[28,29,32] and in tumors of colorectal cancer patients.[33] These cells were shown to display both B-cell helper capacities, and partial cytotoxic functions, but were not extensively characterized.[30,33]

Using a combination of flow cytometry, gene profiling and immunohistochemistry (IHC) in human lymphoma tissues, we describe herein a previously unrecognized subset of CD8 T cells exhibiting phenotypic and functional similarities with T_{FH} cells. This subset was mainly, but not exclusively, associated with cHL tumors.

Materials and methods

Patients

Fresh biopsy lymphoma tissue samples were collected from 86 patients at the time of diagnosis, prior to any treatment. Benign lymphadenitis (n = 8) were used as controls. A part of each sample was mechanically disrupted and passed through a nylon filter (BD Biosciences) to obtain a suspension of dissociated cells, which were immediately frozen for subsequent analysis. The rest of the sample was formalin fixed and paraffin embedded. Hodgkin lymphoma (HL) and B-cell non-HL (NHL) samples were classified according to the World Health Organization (WHO) classification[34] using conventional morphological, immunohistochemical, and clonality analysis. The resulting diagnosis was cHL (n = 43), follicular lymphoma (FL; n = 13), diffuse large B-cell lymphoma (DLBCL; n = 12), marginal zone lymphoma (MZL; n = 3), mantle cell lymphoma (MCL; n = 3), and chronic lymphocytic leukemia (CLL; n = 4). All patients gave informed consent and the study was approved by the ethical board of the Paoli-Calmettes, Albert Bonniot, and Carnot CALYM Institutes.

Cell isolation and purification

CD19$^+$ B cells were obtained from tissues by positive selection using anti-CD19$^+$ microbeads (StemCell Technologies). T cells were then enriched from the unbound fraction by negative selection. To isolate $CD8_{CXCR5+\ ICOS+}$, $CD8_{CXCR5-\ ICOS-}$, and T_{FH} cells for functional assays, enriched T cells were labeled with anti-CD4-phycoerythrin (PE)-Cy7, anti-CD8–Alexa Fluor 700, anti-ICOS-PE, and anti-CXCR5–Alexa Fluor 647 antibodies, together with the viability marker, and sorted by FACSAria (BD Biosciences).

For microarray analysis, $CD8_{CXCR5+\ ICOS+}$ and $CD8_{CXCR5-\ ICOS-}$ T cells isolated from cHL tissues were labeled with anti-CD3-vioblue, anti-CD8-PE, anti CD4-Krome Orange, anti-CXCR5-allophyocyanin (APC) and anti-ICOS-biotin/streptavidin APC-efluor780 before sorting using a FACSAria. In addition, tonsil T_{FH} cells ($CD3^+CD4^+CXCR5^{hi}PD1^{hi}CD25^-CD45RO^+$) and memory CD4$^+$ T cells ($CD3^+CD4^+CXCR5^-PD1^-CD25^-CD45RO^+$) were isolated as previously described.[35]

Surface and intracellular staining

Monoclonal antibodies (mAbs) used are detailed in supplemental Table 1. Cells were surface-stained before fixation/permeabilization and intracellular staining following manufacturer instructions. For perforin and granzyme B, a Cytofix/Cytoperm kit (BD Biosciences) was used whereas a Foxp3 Transcription factor staining buffer set (eBioscience) was used to detect Bcl-6, Eomes, and Ki67 markers. Data were acquired on LSRII (BD Biosciences) and analyzed using FACSDiva and FlowJo software.

Intracellular cytokine secretion

Cells were stimulated with phorbol 12-myristate 13-acetate (20 ng/mL; Sigma) and ionomycin (1 μg/mL; Sigma) in presence of protein transport inhibitor Golgi stop (BD Biosciences) for 5 hours. After stimulation, cells were surface-stained by anti-CD3-ECD (PE-Texas Red), anti-CD4-PE-Cy7, anti-CD8–Alexa Fluor 700, anti-ICOS-PE, anti-CXCR5–Alexa Fluor 488 and live/dead aqua before fixation/permeabilization with the BD Cytofix/cytoperm kit. Cells were washed and stained with intracellular mAbs specific for IL-2, IL-4, IL-10, IL-17, IL-21, IFN-γ, perforin, and granzyme B.

CXCL13 secretion

Sorted T cells were stimulated by phytohemagglutinin (PHA, 2.5 μg/mL; Sigma) in presence of autologous B cells (1:1 ratio) for 48 hours. Culture supernatants were collected to measure CXCL13 secretion using the MILLIPLEX MAP kit (Merck-Millipore) according to the manufacturer's instructions.

CellTrace labeling and T/B proliferation assays

Sorted T cells and CD19$^+$ B cells were stained with CellTrace violet (Life Technologies) following the manufacturer's instructions.

Labeled B- and T-cell subsets were cocultured in presence of PHA (2.5μg/mL) and recombinant human IL-2 (rIL-2; 100 IU/mL) for 5 days with autologous unlabeled T cells or B cells, respectively. For B-cell proliferation, anti-IgM (10 μg/mL; Jackson ImmunoResearch Laboratories) and CpG B (2 μg/mL; Invivogen) were added at the start of the culture in order to activate B cells. Cells were harvested at day 5, stained with anti-CD3-PC7, anti-immunoglobulin D (IgD)-PE, anti-CD38-ECD and live/dead near-infrared. Supernatants were collected to measure IgG secretion by enzyme-linked immunosorbent assay (ELISA) as previously described.[36]

Microarray hybridization data analysis

Microarray analyses were performed on samples of $CD8_{CXCR5+\ ICOS+}$ T cells from cHL (n = 3), $CD8_{CXCR5-\ ICOS-}$ T cells from cHL (n = 3), T_{FH} cells from normal tonsils (n = 3), and memory $CD4^+$ T cells from normal tonsils (n = 3). RNA were amplified and hybridized on GeneChip HTA 2.0 oligonucleotide arrays (Affymetrix), according to the manufacturer's instructions. Expression signal values were obtained for each probe by the Robust Multichip Averaging algorithm using Partek software (Partek Incorporated). A T_{FH} signature comprising all the genes differentially expressed ($P < .05$, I log fold change I > 2) between tonsil T_{FH} cells and tonsil memory $CD4^+$ T cells was obtained using a Student *t* test carried out with Partek software. Similarly, a $CD8_{CXCR5+ICOS+}$ signature comprising all the genes differentially expressed ($P < .05$, I log fold change I > 2) between $CD8_{CXCR5+\ ICOS+}$ and $CD8_{CXCR5-\ ICOS-}$ cells was obtained using a Student *t* test. Gene set enrichment analysis (GSEA) was used to assess the expression of the most variably expressed genes of the T_{FH} signature in cHL $CD8_{CXCR5+\ ICOS+}$ cells vs cHL $CD8_{CXCR5-\ ICOS-}$ cells. A *P* value was calculated for a weighted enrichment score (ES) by using a based permutation test procedure including 1000 permutations.

Immunohistochemistry and clonality analysis

IHC was performed on lymph node whole sections from the paraffin blocks used for diagnosis. After dewaxing and pressure-cooker antigen retrieval, diagnostic phenotyping was performed using anti-CD3, CD4, CD8, ICOS, PD1, CD15, CD20, CD21, and CD30 mAbs, which were incubated in an automated immunostainer (Dako) using a standard avidin biotin peroxidase technique according to the supplier's instructions. For fluorescent dual-color IHC experiments, primary mAbs recognizing ICOS (clone sp98; Abcam), CD8 (clone C8/144B; Dako) and AID (clone mAID-2; Thermo Fisher) were incubated on 2-μm sections for 20 minutes. Secondary antibodies were Alexa 594 and Alexa 488 (Invitrogen), respectively. Slides were then counterstained with 4′,6-diamidino-2-phenylindole and mounted with Vectashield H 1200 mounting medium. If necessary, clonality analysis of the DNA extracted from paraffin blocks was performed using Identiclone TCRB, TCRG, and IGH gene clonality assays (Invivoscribe) according to the supplier's instructions.

Statistical analysis

Quantitative variables were expressed as mean ± standard error of the mean (SEM). Statistical analyses were performed with GraphPad Prism 5 software using the Mann-Whitney nonparametric *U* test and 1-way analysis of variance (*$P \leq .05$; **$P < .01$; ***$P < .001$).

Results

Differential expression of ICOS and CXCR5 defines a distinct subset of CD8 T cells in lymphoma tissues

ICOS, a costimulatory molecule of the CD28 family, is strongly expressed on activated T cells.[37] High ICOS expression on T_{FH} cells is important for their generation and for their B-cell helper activity following engagement with ICOS ligand on B cells.[38-41] We studied ICOS expression on tumor infiltrating-lymphocytes (TIL) using flow cytometry in 86 human lymphoid tissues including 43 cHL, 35 B-NHL and 8 benign samples with reactive hyperplasia. As expected, CD4 T cells were the major subset expressing ICOS among all samples. High numbers of T_{FH} cells defined by CXCR5 and ICOS coexpression were mainly observed in B-NHLs of the follicular type. Interestingly, we found upregulation of ICOS on CD8 T cells in some samples, which also displayed coexpression of ICOS and CXCR5 at high levels (Figure 1A). For further characterization, we have considered these samples as a "$CD8_{CXCR5+\ ICOS+}$-positive" subgroup, defined by a percentage of $CD8_{CXCR5+\ ICOS+}$ T cells 10 times higher than the median value of 0.3% calculated from the 86 analyzed samples.

This subgroup comprised 6 cHL and 1 MZL samples, with a percentage of $CD8_{CXCR5+\ ICOS+}$ cells ranging from 3.6% to 25.1% among CD8 T cells (Figure 1B). These samples also contained a percentage of $CD8_{CXCR5-\ ICOS+}$ cells significantly higher than in other cases (Figure 1C) whereas there was no significant difference in the percentage of $CD8_{CXCR5+\ ICOS-}$ cells (data not shown). There was no specific association between the "$CD8_{CXCR5+\ ICOS+}$-positive" subgroup and B symptoms or viral infection (supplemental Table 2). The 8 benign samples with lymphoid hyperplasia were devoid of $CD8_{CXCR5+\ ICOS+}$ cells. Because high expression of CXCR5 and ICOS[10] is a characteristic feature of T_{FH} cells, we have hypothesized that $CD8_{CXCR5+\ ICOS+}$ T cells could share similarities with T_{FH} cells.

The gene expression profile of $CD8_{CXCR5+\ ICOS+}$ T cells is enriched in T_{FH} genes

The gene expression profile (GEP) of $CD8_{CXCR5+ICOS+}$ and $CD8_{CXCR5-ICOS-}$ TILs were determined using the Affymetrix HTA2.0 microarrays and raw data were normalized with the RMA method. We extracted from our microarray data the $CD8_{CXCR5+ICOS+}$ signature by comparing the GEP of $CD8_{CXCR5+ICOS+}$ and $CD8_{CXCR5-ICOS-}$ subsets. It gathered 2947 and 2750 genes that were over- and underexpressed in $CD8_{\ CXCR5+ICOS+}$ cells, respectively. In the same way, we obtained the T_{FH} signature by comparison between tonsil-sorted $CD3^+CD4^+CXCR5^{hi}PD1^{hi}CD25^-CD45RO^+$ T_{FH} cells and memory T cells. This T_{FH} signature comprised 4181 genes, representing 2056 upregulated genes, and 2125 downregulated genes. When we focused on the genes that were underexpressed in both T_{FH} and $CD8_{CXCR5+ICOS+}$ signatures, we found 932-shared genes (Figure 2A; supplemental Table 3). Similarly, we highlighted 885 genes that were upregulated in the two signatures (Figure 2B; supplemental Table 4). Among them, we confirmed the high expression of CXCR5 and ICOS, and noticed the presence of typical human T_{FH} markers, like BCL6, SH2D1A, MAF, CD200, CXCL13, IL21, BTLA. Of note, our $CD8_{CXCR5+ICOS+}$ signature did not show any enrichment in genes involved in the IL-6 or TCF-1 pathways which have been shown to

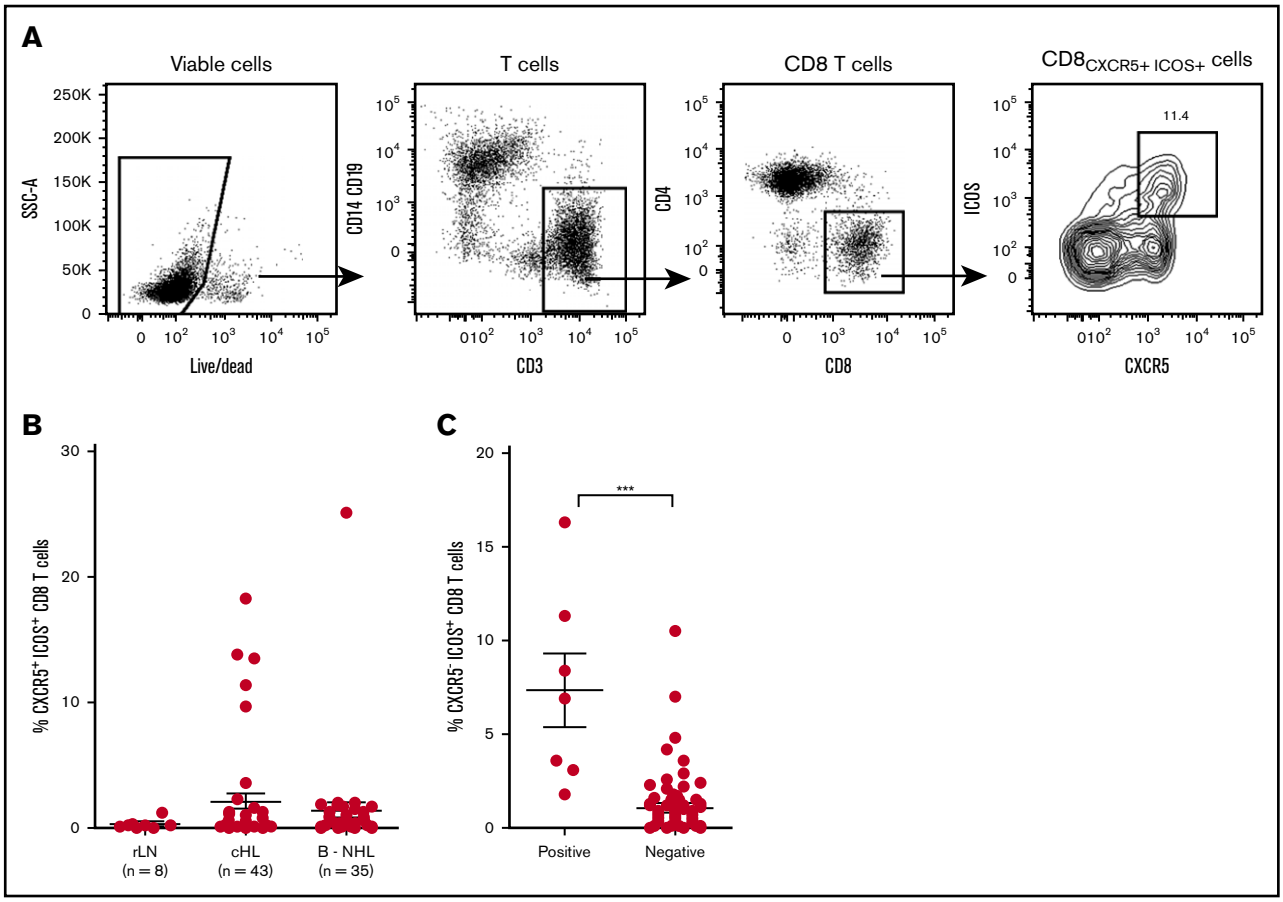

Figure 1. Identification of $CD8_{CXCR5+ICOS+}$ T cells in human lymphoma tissues. Frozen cells isolated from lymphoma biopsy samples were analyzed by flow cytometry. (A) Gating strategy to identify the $CD8_{CXCR5+ICOS+}$ subset. CD8 T cells were identified from viable CD3 T cells (live/dead-negative CD14 $CD19^{-}CD3^{+}$), then CXCR5 and ICOS coexpression was defined among viable CD8 T cells. (B) Percentage of $CD8_{CXCR5+ICOS+}$ cells among CD8 T cells in different lymphoma samples. (C) Percentage of $CD8_{CXCR5-ICOS+}$ among CD8 T cells in cases containing $CD8_{CXCR5+ICOS+}$ cells (positive subgroup), compared with cases lacking $CD8_{CXCR5+ICOS+}$ cells (negative subgroup). ***$P < .001$.

guide helper CD8 T cells generation in vitro[42] and in viral infection model[27,28] respectively (data not shown).

To evaluate the enrichment of classical T_{FH} genes in $CD8_{CXCR5+ICOS+}$ compartment, we performed a GSEA using the 406 most variably expressed genes of the T_{FH} signature (CV > 15%; supplemental Table 5). Interestingly, we found that the $CD8_{CXCR5+ICOS+}$ GEP was significantly enriched in genes expressed in this specific T_{FH} signature ($P < .01$, FDR < 0.25, enrichment score = 0.45; Figure 2C). Moreover, we found that this set of 406 genes was sufficient to cluster together $CD8_{CXCR5+ICOS+}$ T cells and T_{FH} cells versus memory CD4 T cells and $CD8_{CXCR5-ICOS-}$ cells (Figure 2D).

$CD8_{CXCR5+\ ICOS+}$ T cells share phenotypic markers with T_{FH} cells

$CD8_{CXCR5+\ ICOS+}$ T cells were analyzed by flow cytometry and compared with both $CD8_{CXCR5-\ ICOS-}$ and T_{FH} cells, all gated among TILs from the 6 cHL cases containing $CD8_{CXCR5+\ ICOS+}$ cells. We observed that most $CD8_{CXCR5+\ ICOS+}$ cells were $CD45RA^{-}$ $CD27^{+}$, providing a central memory phenotype (supplemental Figure 1). Like T_{FH} cells, $CD8_{CXCR5+\ ICOS+}$ cells displayed scant CCR7 expression (mean ± SEM: 5.1% ± 1.1% and 6.3% ± 1.9% for $CD8_{CXCR5+\ ICOS+}$ and T_{FH}, respectively vs 42.3 ± 8% for $CD8_{CXCR5-\ ICOS-}$, $P = .007$, n = 5) (Figure 3A). When compared with the $CD8_{CXCR5-\ ICOS-}$ subset, $CD8_{CXCR5+ICOS+}$ cells highly expressed T_{FH}-associated markers like PD1 and BTLA (80.5 ± 6% vs 15.1 ± 2.6%, $P = .002$, n = 6) (Figure 3B top), Bcl-6 (32.8 ± 6.7% vs 1.8 ± 0.2%, $P = .002$, n = 6) and other effector molecules such as OX40 (17 ± 5.7% vs 1.7 ± 0.3%, $P = .01$, n = 5) and CD200 (66.2 ± 6.4% vs 10.6 ± 1.7%, $P = .007$, n = 5) (Figure 3B bottom).

In addition, both subsets of $CD8_{CXCR5+ICOS+}$ and T_{FH} cells significantly upregulated the activation marker HLA-DR and the proliferation marker Ki67 (Figure 3C). In contrast, expression of markers associated with CD8 effector functions including perforin, granzyme B and Eomes[43] was lower in $CD8_{CXCR5+\ ICOS+}$ cells compared with $CD8_{CXCR5-\ ICOS-}$ cells (Figure 3D). These results suggest a T_{FH}-like phenotype and a decreased cytotoxic function of $CD8_{CXCR5+\ ICOS+}$ cells.

$CD8_{CXCR5+\ ICOS+}$ T cells display a functional profile evocative of T_{FH} properties

Intracellular secretion of IL-2, IL-4, IL-10, IL-17, IFN-γ, perforin and granzyme B following stimulation was analyzed in $CD8_{CXCR5+\ ICOS+}$ cells, in comparison with $CD8_{CXCR5-ICOS-}$ and T_{FH} cells (Figure 4A-B;

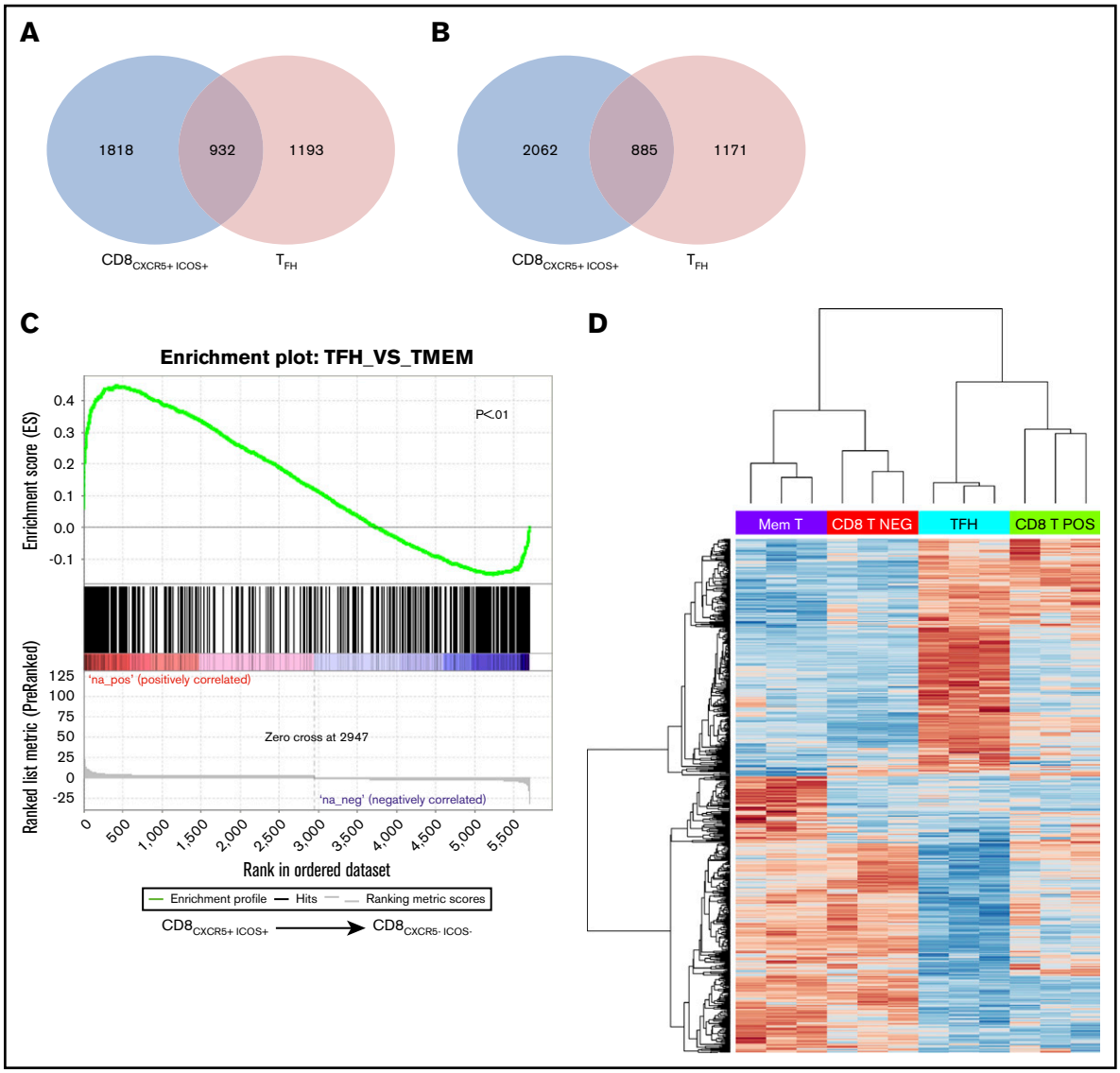

Figure 2. $CD8_{CXCR5+ICOS+}$ gene expression profile. (A) Venn diagram allowing the retrieval of shared downregulated genes between the $CD8_{CXCR5+ICOS+}$ (blue) and T_{FH} (red) signatures. (B) Venn diagram allowing the retrieval of shared upregulated genes between the $CD8_{CXCR5+ICOS+}$ (blue) and T_{FH} (red) signatures. (C) Gene set enrichment score curves for T_{FH} signature in $CD8_{CXCR5+ICOS+}$ and $CD8_{CXCR5-ICOS-}$ cell subsets. Vertical black lines indicate the position of genes included in the specific T_{FH} signature. (D) Heatmap representation of the 406 most variably expressed genes of the T_{FH} signature for memory $CD4^+$ T cells (Mem T), T_{FH} cells, $CD8_{CXCR5+ICOS+}$ cells (CD8 T NEG), and $CD8_{CXCR5+ICOS+}$ cells (CD8 T POS).

supplemental Figure 2). The $CD8_{CXCR5+\ ICOS+}$ subset mostly produced IL-2, IL-4 and IL-21 (supplemental Figure 2). The profile was similar to T_{FH} cells, especially for cytokines known to strongly support B-cell responses, ie, IL-4 and IL-21 (Figure 4A). In contrast, the secretion of cytotoxic effectors like perforin, granzyme B and IFN-γ was weak in $CD8_{CXCR5+\ ICOS+}$ cells (supplemental Figure 2), and even lower than in $CD8_{CXCR5-\ ICOS-}$ cells (Figure 4B). $CD8_{CXCR5+\ ICOS+}$ cells secreted CXCL13 as strongly as T_{FH} cells in response to PHA stimulation in presence of autologous B cells (Figure 4C).

Because recent reports have suggested that T_{FH} have limited proliferative capacity,[41] we analyzed the proliferation of $CD8_{CXCR5+\ ICOS+}$ cells in comparison with other T cells subsets. At day 5, most $CD8_{CXCR5-\ ICOS-}$ cells had undergone proliferation, whereas limited proliferation was observed in both $CD8_{CXCR5+\ ICOS+}$ and T_{FH} subsets (mean ± SEM of DI: 1.2 ± 0.12; 0.3 ± 0.14 and 0.36 ± 0.09 for $CD8_{CXCR5-\ ICOS-}$, $CD8_{CXCR5+\ ICOS+}$ and T_{FH}, respectively, $P = .002$). A similar result was observed as to the cell survival capacity. After 5 days of stimulation, the average survival rate was less than 45% for $CD8_{CXCR5+ICOS+}$ and T_{FH} cells (43% ± 12 and 44% ± 12 respectively), whereas it was close to 70% in $CD8_{CXCR5-ICOS-}$ cells (70.8% ± 7.5) (Figure 4D).

Altogether these data demonstrate that, by comparison with $CD8_{CXCR5+ICOS-}$ and $CD8_{CXCR5-ICOS+}$ cells, $CD8_{CXCR5+ICOS+}$ cells hardly produce cytotoxic molecules (supplemental Table 6). In contrast, they share many phenotypic and functional characteristics with T_{FH} cells. This led us to postulate that the $CD8_{CXCR5+ICOS+}$ subset may be able to support follicular B cells.

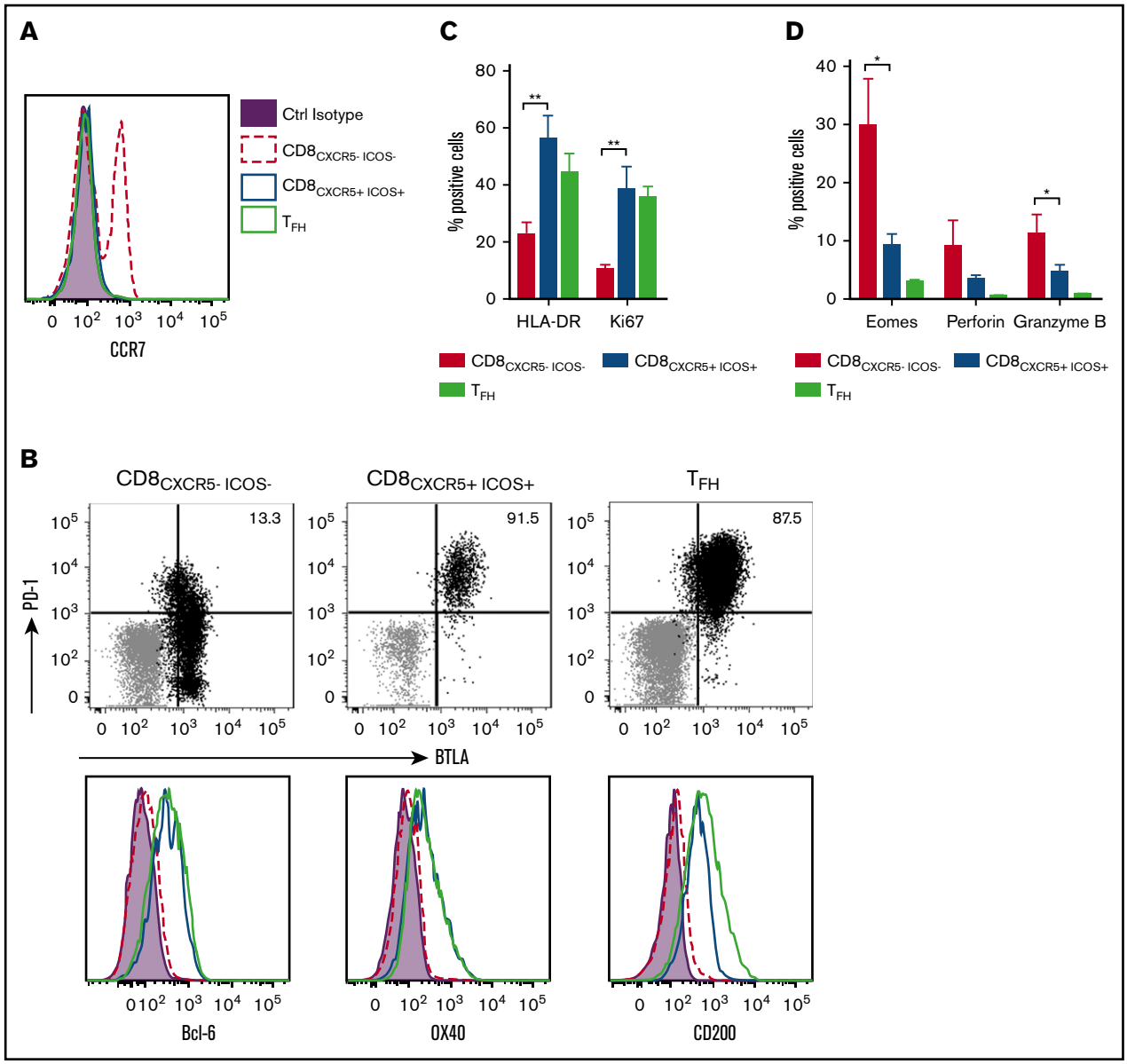

Figure 3. Phenotypic characterization of $CD8_{CXCR5+ICOS+}$ T cells. Expression of various markers was analyzed by flow cytometry in $CD8_{CXCR5+ICOS+}$ cells compared with $CD8_{CXCR5-ICOS-}$ and T_{FH} subsets (n = 5-6). Representative figures from 1 cHL case are shown for expression of chemokine receptor CCR7 (A), PD1 and BTLA coexpression (black) vs isotype control (gray) (B, top), transcription factor Bcl-6 and effector molecules like OX40, CD200 (B, bottom). (C) Percentage of cells positive for the activation marker HLA-DR and the proliferation marker Ki67. (D) Percentage of cells positive for perforin, granzyme B, and Eomes in each cell subset. Statistical analyses using the Mann-Whitney nonparametric *U* test between $CD8_{CXCR5+ICOS+}$ compared with $CD8_{CXCR5-ICOS-}$ cell subsets are shown (*$P < .05$; **$P < .01$).

$CD8_{CXCR5+\ ICOS+}$ T cells are capable of supporting B cells

In order to test whether $CD8_{CXCR5+\ ICOS+}$ cells were able to support B cells, $CD8_{CXCR5+\ ICOS+}$, $CD8_{CXCR5-\ ICOS-}$ and T_{FH} cells were sorted and cocultured with autologous $CD19^+$ B cells, most of which being naïve cells (supplemental Figure 3), in presence of PHA and B-cell stimulators like anti-IgM and CpG-B. To evaluate B-cell proliferation, $CD19^+$ B cells were labeled with CellTrace violet prior coculture. Coculture with either $CD8_{CXCR5+\ ICOS+}$ or T_{FH} cells had a tendency to induce a higher B cells proliferation compared with $CD8_{CXCR5-\ ICOS-}$ cells, despite a marked heterogeneity between the 3 samples analyzed, (mean ± SEM of DI: 0.79 ± 0.12; 1.15 ± 0.08 and 1.16 ± 0.07 for $CD8_{CXCR5-\ ICOS-}$, $CD8_{CXCR5+\ ICOS+}$ and T_{FH}, respectively, $P = .06$) (Figure 5A). We have evaluated the percentage of different B cells subsets by CD38 and IgD staining as previously described.[44] Like T_{FH} cells, $CD8_{CXCR5+ICOS+}$ cells had a tendancy to increase the number of $IgD^-CD38^{+/-}$ B cells (mean ± SEM: 18.7% ± 7.7; 32% ± 3.6 and 50.8% ± 14.2 for $CD8_{CXCR5-\ ICOS-}$, $CD8_{CXCR5+\ ICOS+}$ and T_{FH}, respectively, $P = .1$). Significantly higher proliferation rates were observed among $IgD^-\ CD38^{+/-}$ B cells in coculture with either $CD8_{CXCR5+ICOS+}$ or T_{FH} cells (mean ± SEM: 0.51 ± 0.23; 1.2 ± 0.06 and 1.3 ± 0.3 for $CD8_{CXCR5-\ ICOS-}$, $CD8_{CXCR5+\ ICOS+}$ and

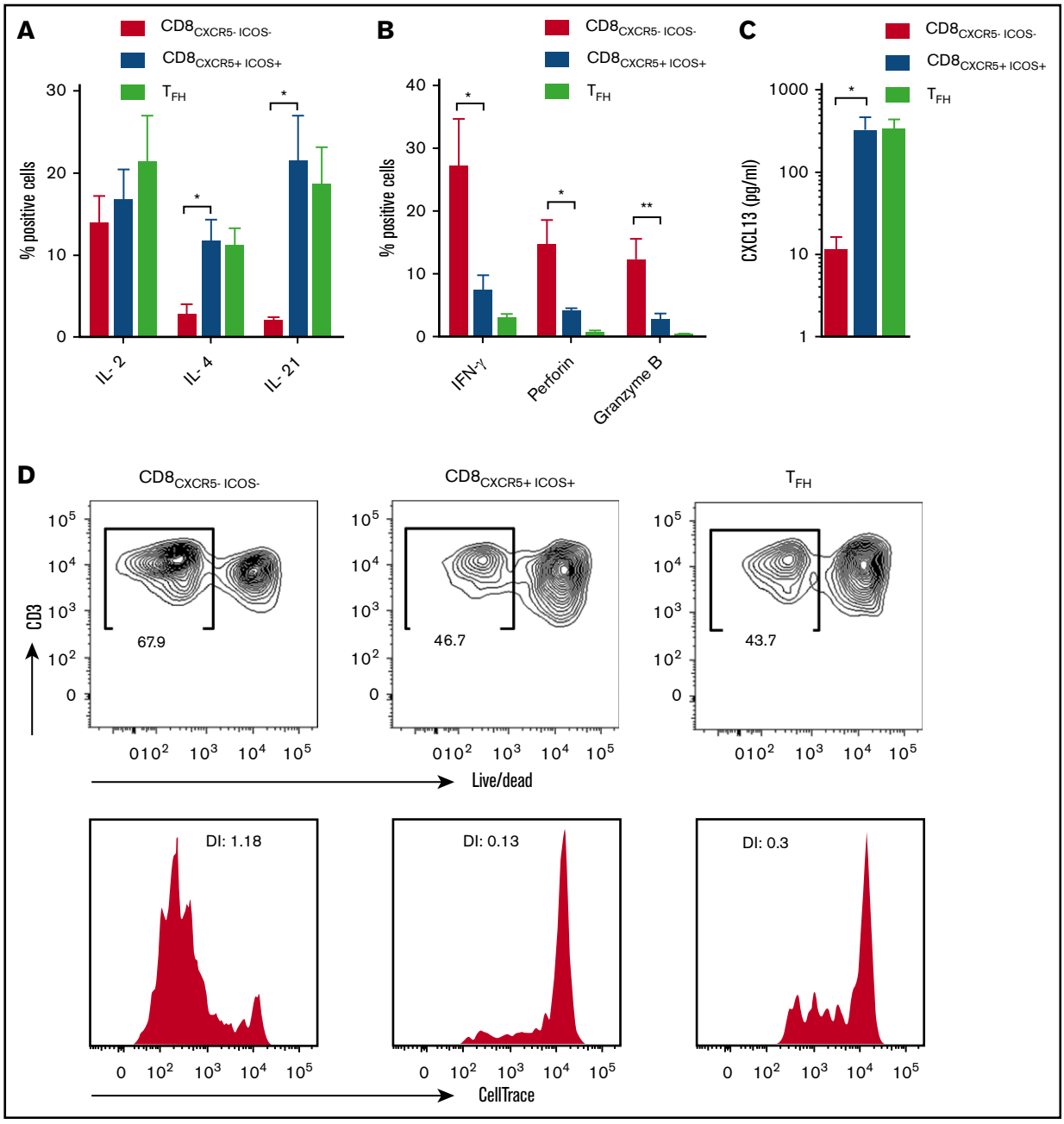

Figure 4. Functional characterization of $CD8_{CXCR5+ICOS+}$ T cells. (A-B) Cells isolated from lymphoma tissues were stimulated by phorbol 12-myristate 13-acetate/iono in presence of the protein transport inhibitor Golgi Stop. Intracellular cytokine secretion was analyzed in each T-cell subset (n = 4-6). (C) CXCL13 secretion measured by Luminex in the supernatant of each sorted T-cell subset after coculture with autologous B cells in presence of PHA for 48 hours (n = 4). (D) Representative dot plots and histograms for survival (top) and proliferative capacity (bottom) of each T-cell subset after coculture with autologous B cells for 5 days in presence of PHA (results from 3 independent experiments). Survival and proliferation were evaluated by the percentage of lived/dead-negative cells and division index (DI), respectively. The Mann-Whitney nonparametric *U* test (*$P < .05$; **$P < .01$) was performed.

T_{FH}, respectively, $P = .01$) (Figure 5B). Accordingly, the percentages of naïve B cells (IgD^+CD38^-) in coculture with $CD8_{CXCR5+\ ICOS+}$ (and T_{FH} cells as well) were low (mean ± SEM: 27% ± 4.1; 12% ± 4.4 and 8.2% ± 3.7 for $CD8_{CXCR5-\ ICOS-}$, $CD8_{CXCR5+\ ICOS+}$ and T_{FH}, respectively, $P = .01$) (Figure 5B). No significant variation was observed as to the percentages of activated IgD^+CD38^+ naïve B cells (mean ± SEM: 53.03 ± 7.6; 54.4 ± 7.2 and 40.3 ± 11 for $CD8_{CXCR5-\ ICOS-}$, $CD8_{CXCR5+\ ICOS+}$ and T_{FH}, respectively $P = .5$) (Figure 5B).

We next measured the influence of $CD8_{CXCR5+\ ICOS+}$ on IgG production by B cells in supernatants. Coculture of B cells with $CD8_{CXCR5+\ ICOS+}$ cells induced a twofold increase in IgG production when compared with $CD8_{CXCR5-\ ICOS-}$ cells ($P = .08$) (Figure 5C). Coculture with $CD8_{CXCR5-ICOS-}$ cells resulted not only in low IgG production, but also in B cells with low proliferation. Altogether, these results suggest that $CD8_{CXCR5+\ ICOS+}$ cells are able to support B-cell responses in vitro.

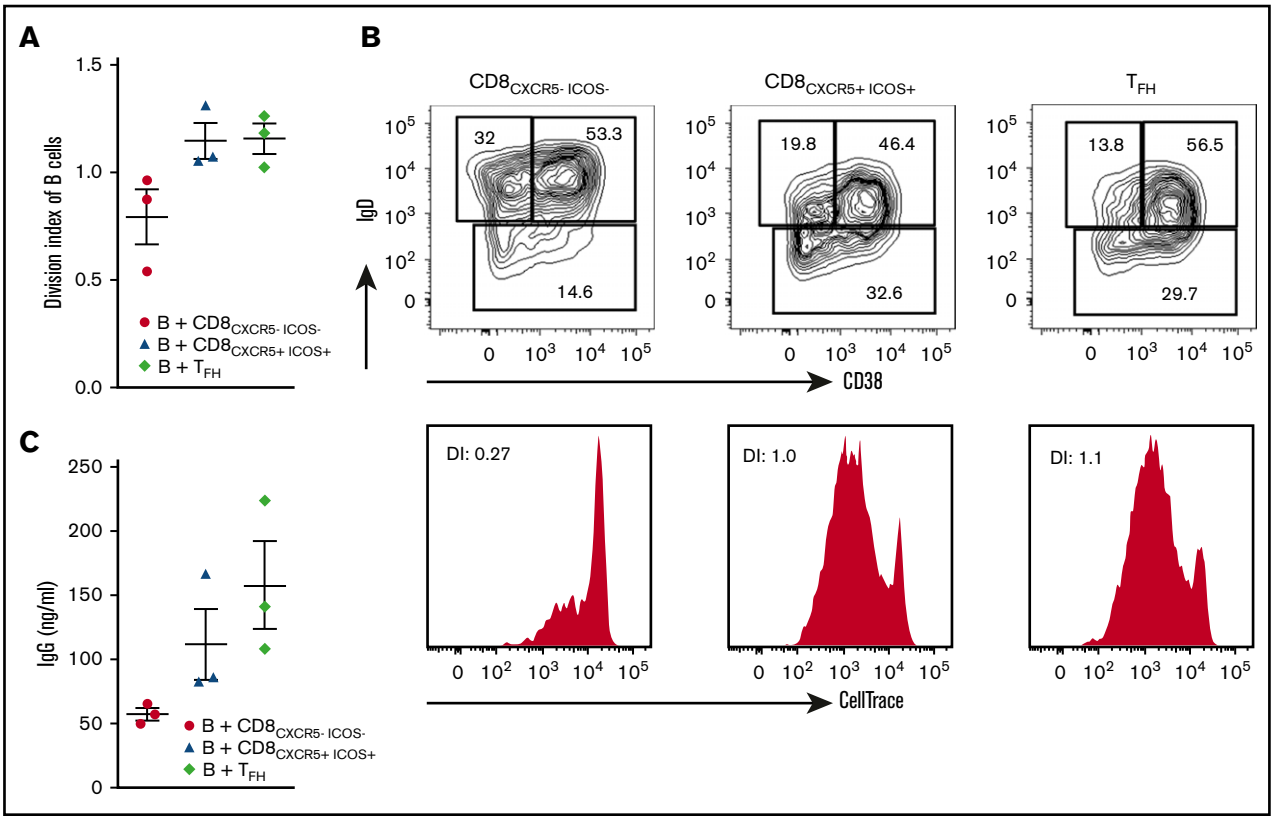

Figure 5. Functional effects of $CD8_{CXCR5+ICOS+}$ T cells. Cell Trace–labeled purified B cells from lymphoma tissues were activated by anti-BCR and CpG and cocultured with autologous sorted T cells in presence of PHA and IL-2 for 5 days (n = 3). (A) Proliferation of B cells evaluated by DI in each condition. (B) Representative dot plots and histograms for percentages of IgD^+CD38^-, IgD^+CD38^+, and $IgD^-CD38^{+/-}$ cells among viable B cells (top) and proliferation rate of $IgD^-CD38^{+/-}$ B cells (bottom) after 5 days of coculture in each condition. (C) IgG production measured in supernatant at day 5 by ELISA. A 1-way ANOVA statistic test was done.

Lymphoma tissues with $CD8_{CXCR5+\ ICOS+}$ T cells share common histophenotypical features

The 43 cHL samples analyzed, including the 6 samples with $CD8_{CXCR5+ICOS+}$ cells, fulfilled the WHO diagnostic criteria for cHL[34] including the presence of $CD30^+/CD15^+/CD20^-$ RS cells admixed with an abundant inflammatory cell component. The 6 cHL cases with $CD8_{CXCR5+\ ICOS+}$ cells closely resembled the cHL subtype referred to as "nodular lymphocyte rich cHL" (NLRcHL)[34] due to a nodular architectural pattern without significant sclerosis (Figure 6A-B) and the presence of residual GCs. However, in contrast with the small or regressed GCs usually observed in NLRcHL,[34] residual GCs in our 6 cases were mostly hyperplastic, although they exhibited various degrees of destruction by the surrounding tumor cells (Figure 6C-E). Of note, some RS cells could be observed in close vicinity of GC cells (Figure 6D-E), a feature which is considered as exceptional in NLRcHL.[34] Eosinophils were focally present (Figure 6F), which is also not a typical feature of NLRcHL.[34] EBV was detected in 3/6 cases (supplemental Table 2).

The IHC phenotypic profile of cHL cases with $CD8_{CXCR5+ICOS+}$ cells was reminiscent of that observed in NLRcHL, due to a major content of small B-lymphocytes and scarce RS cells (Figure 6F) with $PD1^+/CD4^+$ T-cell rosetting. Most tumor nodules were considered as CD8-poor, because they contained rare CD8 T cells, (Figure 6G G2), together with scant $ICOS^+$ cells (Figure 6H H2) and scarce neoplastic cells (Figure 6G G2; Figure 6H H2). In contrast, other tumor nodules, considered as CD8-rich, harbored a high content of CD8 T cells (Figure 6G), associated with high numbers of $ICOS^+$ cells (Figure 6H) and numerous RS cells (Figure 6G G1; Figure 6H H1). CD8/ICOS co-expression could be evidenced by double-staining experiments (Figure 6I). Overall, cHL tumors with $CD8_{CXCR5+\ ICOS+}$ cells were uneasy to be strictly classified as NLRcHL due to their cytological and phenotypical heterogeneity within a given sample, a pattern that we called "mixed nodularity". Such a pattern was not observed in the 37 cHL cases which lacked $CD8_{CXCR5+\ ICOS+}$ cells, including 3 typical NLRcHL samples. Beside cHL cases, only 1 of 35 B-NHLs analyzed contained $CD8_{CXCR5+ICOS+}$ cells. This was an unusual B-cell MZL case with follicular hyperplasia.

AID immunostaining showed only rare AID positive cells (<1 cell per high power field) in the tumor areas of 4 cHL cases devoid of $CD8_{CXCR5+\ ICOS+}$ cells (supplemental Figure 4A- B). In contrast, the 4 analyzed samples with $CD8_{CXCR5+\ ICOS+}$ cells contained higher numbers of AID positive cells (from 5 to 15 cells per high power field), located in CD8-rich areas close to neoplastic cells (supplemental Figure 4C-D). Of note, the highest level of AID positivity was observed in the case displaying the highest amount of $CD8_{CXCR5+\ ICOS+}$ cells (supplemental Figure 4E-F). In all analyzed cases, the residual germinal centers did not exhibit any difference in the intensity of AID positivity, whereas AID positive cells outside the GCs showed an immunoblastic appearance (supplemental Figure 4).

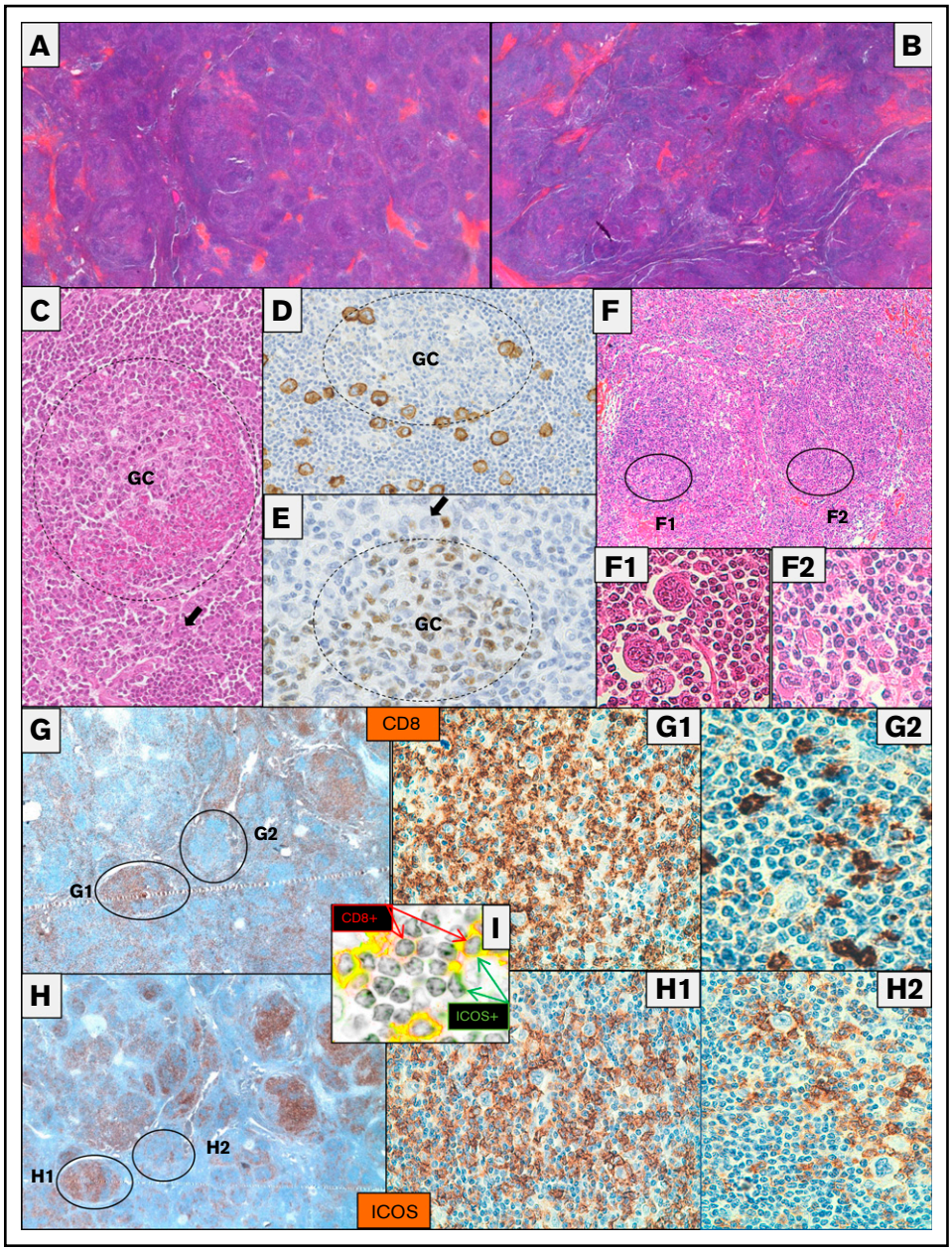

Figure 6. Histological and immunohistochemical features of cHL cases with $CD8_{CXCR5+ ICOS+}$ T cells. Low power views (hematoxylin and eosin [H&E] stain, original magnification ×25) of 2 different cHL cases with $CD8_{CXCR5+ ICOS+}$ cells show a similar pattern of nodular architecture, with only scant fibrotic foci (A-B). There was no nodular sclerosis. A variable number of hyperplastic and/or disrupted GCs were present (C, original magnification ×100; H&E stain), and surrounded by neoplastic Reed-Sternberg (RS) cells (C, arrow). CD30 (D, original magnification ×100) and Bcl-6 (E, original magnification ×400) immunostainings highlighted the close vicinity between neoplastic cells ($CD30^+$ cells in panel D and arrow in panel E) and GC cells, whereas the mantle zone was deficient (dotted circle on panels C-E). The cell composition of most nodules included a majority of reactive lymphocytes and scattered RS cells (F, original magnification ×50; F1, original magnification ×400; H&E stain), though some eosinophils could be focally observed (F2, original magnification ×400; H&E stain). A few nodules considered as CD8-rich contained high numbers of $CD8^+$ cells surrounding numerous RS cells (G, original magnification ×25; G1, original magnification ×200). However, most nodules were considered as CD8-poor, because they contained only scarce CD8 T cells (G; G2, original magnification ×400). ICOS immunostaining (H, original magnification ×25) on a serial section showed that CD8-rich nodules displayed strong ICOS expression (H1, original magnification ×200), whereas ICOS expression was weak in CD8-poor nodules (H2, original magnification ×200) with a distribution evocative of CD4 T_{FH} rosetting. Double fluorescent immunostaining (panel I, original magnification ×600) shows ICOS (green) and CD8 (red) coexpression at a single-cell level (yellow) in CD8-rich nodules.

Hence, it is noteworthy that the common feature of lymphoma samples with $CD8_{CXCR5+ ICOS+}$ cells was the presence of hyperplastic GCs with various degrees of destruction by tumor cells focally associated with CD8 T cells (supplemental Figure 5).

As to clinical correlations, these cases presented as low-stage (I-II) tumors without B symptoms, but complete remission was not achieved for all patients (supplemental Table 2).

Discussion

We describe herein a previously unrecognized subset of $CD8_{CXCR5+ICOS+}$ T cells reminiscent of T_{FH} cells. In fact, these T cells display a phenotypic profile mimicking T_{FH} cells, due to high expression of ICOS, CXCR5, Bcl-6, PD1, BTLA, OX40, and CD200, together with scant CCR7 expression. $CD8_{CXCR5+ICOS+}$ T cells show failure of CD8 canonical functions such as secretion of cytolytic molecules and IFN-γ, whereas they produce T_{FH}-associated cytokines like IL-4, IL-21, and CXCL13. In addition, they are able to support B-cell proliferation and IgG production as efficiently as CD4 T_{FH} cells.

This particular human CD8 T-cell subset is also reminiscent of $CXCR5^+$ CD8 T cells previously identified in mice and sharing similarities with T_{FH} cells.[27-29] These cells were shown to migrate into B-cell follicles where they could eradicate virus-infected T_{FH} and B cells.[28,29] In addition, a subset of IL-21–producing CD8 T cells with B-cell helper capacities has been observed in mice during influenza infection and could be induced by IL-6 in vitro.[42] These CD8 T cells were shown to favor the production of virus-specific IgG antibodies during virus infection.[42] As to humans, $CD8_{CXCR5+}$ T cells were previously described in human benign tonsils, with a modest capacity to support B cells, but without ICOS expression.[30] Our results confirm that $CD8_{CXCR5+\ ICOS-}$ T cells are commonly found not only in human reactive lymphoid tissues, but also in lymphoma tumors. Furthermore, we report for the first time a particular $CD8_{CXCR5+\ ICOS+}$ subset. This subset appears uncommon because it was present in only 7 of 78 lymphoma samples, whereas it was absent from nonneoplastic samples. Furthermore, $CD8_{CXCR5+\ ICOS+}$T cells are phenotypically and functionally different from $CD8_{CXCR5+\ ICOS-}$ T cells.

Several nonmutually exclusive mechanisms could explain the expression of both ICOS and CXCR5 in intratumoral CD8 cells. It is well known that T cells expressing high levels of CXCR5 together with low levels of CCR7 are prone to be localized into B-cell follicles.[45] Because $CD8_{CXCR5+\ ICOS+}$ cells fulfill these criteria, they are likely to be at least transiently in contact with GC cells. In line with this hypothesis, a common point shared by lymphoma tissues with $CD8_{CXCR5+\ ICOS+}$ cells was the presence of residual GCs partly disrupted by the surrounding tumor infiltrate, including neoplastic cells and reactive T cells. Hence, CXCR5 expression may be acquired by some $CD8_{CXCR5-\ ICOS+}$ cells as a consequence of their coincidental vicinity with residual GC cells. The presence of $CD8_{CXCR5+\ ICOS+}$ cells within the tumor microenvironment may in turn favor hyperplasia of residual GCs, as suggested by our finding that $CD8_{CXCR5+\ ICOS+}$ cells are able to support B-cell proliferation and differentiation. Besides, our observation of higher numbers of AID^+ cells in tissue samples containing $CD8_{CXCR5+\ ICOS+}$ cells suggests a possible IL-21–induced AID overexpression in these tumors.

Alternatively, the high expression of activation markers by $CD8_{CXCR5+ICOS+}$ cells compared with $CD8_{CXCR5+\ ICOS-}$ cells suggests that $CD8_{CXCR5+\ ICOS+}$ cells may correspond to an activation state of $CD8_{CXCR5+}$ cells. This is in line with a previous study showing that ICOS can be upregulated in $CD8_{CXCR5+}$ cells upon in vitro activation.[30] Because we have also found a significant component of $CD8_{CXCR5-\ ICOS+}$ cells in all samples harboring $CD8_{CXCR5+\ ICOS+}$ cells, it is possible that a global activation process of CD8 T cells may have occurred in these tumors.

In contrast with $CD8_{CXCR5+ICOS+}$ which were devoid of cytotoxic activity, stimulated $CD8_{CXCR5-\ ICOS+}$ cells strongly expressed IFN-γ, granzyme B, and perforin together with activation markers. $CD8_{CXCR5-\ ICOS+}$ cells thus fulfill the criteria of activated cytotoxic effectors able to react against tumor cells. Hence it is possible that an unusual antitumor reaction involving $CD8_{CXCR5-\ ICOS+}$ cells could occur in rare lymphoma tumors. Cytotoxic $CD8_{CXCR5-ICOS+}$ cells could then interact with residual GCs to acquire T_{FH} features and become $CD8_{CXCR5+\ ICOS+}$ cells. To this extent, the CD8 activation process associated with ICOS expression could be the initial event of a putative immunoediting in lymphoma tissues, with CXCR5 expression occurring only as a secondary event. However, we cannot exclude that $CD8_{CXCR5+\ ICOS+}$ cells could also exert a protumor effect by direct stimulation of RS cells which are known to express the IL21 receptor.[46]

The observation that cHL is the main lymphoma subtype harboring both $CD8_{CXCR5+ICOS+}$ and $CD8_{CXCR5-\ ICOS+}$ cell subsets is in accordance with previous data showing dynamic CD8 T cells responses in cHL patients.[47] Of note, these responses were reported against tumor-associated EBV antigens, even in patients with EBV^- HL.[47] In our series, HL cases with T_{FH}-like CD8 cells did not show any correlation with EBV infection. They presented as low-stage tumors without B symptoms, but complete remission was not achieved for all patients. The number of cases, however, is too small to draw a final conclusion as to putative correlations with clinical parameters.

The histopathological pattern of cHL tumors harboring $CD8_{CXCR5+\ ICOS+}$ cells was characterized by a nodular architecture without sclerosis, which was reminiscent of the NLRcHL subtype.[33] This subtype is associated with a slightly better prognosis than that of the other cHL subtypes,[33] which is in accordance with the hypothesis of a better antitumor response. The presence of residual GCs admixed with tumor nodules is a rare event in cHL, and is mainly observed in the NLRcHL subtype.[34,48] Nonetheless, our cHL cases with $CD8_{CXCR5+\ ICOS+}$ cells somewhat differed from NLRcHL due to their cytological and phenotypical heterogeneity, resulting in a global appearance of "mixed nodularity." Besides, among the 37 cHL cases devoid of $CD8_{CXCR5+\ ICOS+}$ cells, there were 3 cases of NLRcHL subtype, which suggests that this subtype is not strictly correlated with the presence of $CD8_{CXCR5+\ ICOS+}$ cells. It appears eventually that cHL tumors with $CD8_{CXCR5+ICOS+}$ cells are uneasy to classify in the current WHO lymphoma classification. Larger series are needed to determine whether the "mixed nodularity" pattern could be considered as a variant of NLRcHL, or just reflects a potential plasticity of cHL lesions.

In summary, the present study identifies a previously unknown CD8 T-cell subset with T_{FH} features, which may be related to an unusual, CD8-mediated, antitumor reaction, mainly acting in particular cHL tumors. Although larger cohorts are needed to understand the influence of this putative immunoediting on the course of the disease, these data open insights toward the development of therapies aiming to modulate ICOS-related CD8 activation in the tumor microenvironment.

Acknowledgments

The authors thank the cytometry platforms (Centre de Recherche en Cancérologie de Marseille–INSERM U1068, Marseille, France and Unité Mixte de Service Centre National de la Recherche Scientifique [CNRS] 3480/US INSERM 018 Biologie, Santé,

Innovation Technologique [BIOSIT], Rennes, France), the microarray and sequencing platform (Institut de Génétique et de Biologie Moléculaire et Cellulaire, Strasbourg, France), the Infrastructures en Biologie Santé et Agronomie [IBiSA] Cancer Immunotoring Platform and the Department of Biopathology (Institut Paoli-Calmettes) for their help. The authors also thank Paoli-Calmettes, Albert Bonniot, and Carnot Consortium pour L'Accélération de L'Innovation et de son Transfert dans le Domaine du Lymphome (CALYM) Institute for collection of biologic samples as well as all patients for their agreements to be involved in this study.

This work was supported by grants from Institut National du Cancer (INCa; 2013-085), Agence Nationale de la Recherche (ANR), the pharmaceutical company GlaxoSmithKline, and by fellowships (K.-S.L.) from Ministère de l'Enseignement Supérieur et de la Recherche and the Ligue Nationale contre le Cancer. D.O.'s team was labeled Equipe FRM DEQ 201 40329534. Cell collection was obtained through the CeVi Collection Project from the CALYM Carnot Institute funded by the ANR. D.O. is Senior Scholar of the Institut Universitaire de France.

Authorship

Contribution: K.-S.L. designed the research, performed experiments, analyzed and interpreted data, and wrote the paper; P.A.-T. and K.T. contributed to the design of project research, performed and interpreted microarray experiments, and helped writing the paper; F.G.-R., S.G., F.O., and E.D.F. contributed to analysis and interpretation of data, F.B., R.B., T.F., D.L., S.Y., and P.A.M. contributed to the design of project research; L.X. designed the project research, performed and interpreted the IHC experiment, and helped writing the paper; and D.O. designed the project research, contributed to data interpretation, and helped writing the paper.

Conflict-of-interest disclosure: D.O. is cofounder of Imcheck Therapeutics. The remaining authors declare no competing financial interests.

Correspondence: Daniel Olive, Centre de Recherche en Cancérologie de Marseille, CNRS U7258/INSERM U1068, Aix Marseille Université, Institut Paoli-Calmettes, 27 Bd Lei Roure, 13009 Marseille, France; e-mail: daniel.olive@inserm.fr.

References

1. Scott DW, Gascoyne RD. The tumour microenvironment in B cell lymphomas. *Nat Rev Cancer*. 2014;14(8):517-534.
2. Küppers R, Engert A, Hansmann ML. Hodgkin lymphoma. *J Clin Invest*. 2012;122(10):3439-3447.
3. Steidl C, Connors JM, Gascoyne RD. Molecular pathogenesis of Hodgkin's lymphoma: increasing evidence of the importance of the microenvironment. *J Clin Oncol*. 2011;29(14):1812-1826.
4. Alvaro-Naranjo T, Lejeune M, Salvadó-Usach MT, et al. Tumor-infiltrating cells as a prognostic factor in Hodgkin's lymphoma: a quantitative tissue microarray study in a large retrospective cohort of 267 patients. *Leuk Lymphoma*. 2005;46(11):1581-1591.
5. Chetaille B, Bertucci F, Finetti P, et al. Molecular profiling of classical Hodgkin lymphoma tissues uncovers variations in the tumor microenvironment and correlations with EBV infection and outcome. *Blood*. 2009;113(12):2765-3775.
6. Steidl C, Lee T, Shah SP, et al. Tumor-associated macrophages and survival in classic Hodgkin's lymphoma. *N Engl J Med*. 2010;362(10):875-885.
7. Greaves P, Clear A, Owen A, et al. Defining characteristics of classical Hodgkin lymphoma microenvironment T-helper cells. *Blood*. 2013;122(16):2856-2863.
8. Breitfeld D, Ohl L, Kremmer E, et al. Follicular B helper T cells express CXC chemokine receptor 5, localize to B cell follicles, and support immunoglobulin production. *J Exp Med*. 2000;192(11):1545-1552.
9. Schaerli P, Willimann K, Lang AB, Lipp M, Loetscher P, Moser B. CXC chemokine receptor 5 expression defines follicular homing T cells with B cell helper function. *J Exp Med*. 2000;192(11):1553-1562.
10. Crotty S. Follicular helper CD4 T cells (TFH). *Annu Rev Immunol*. 2011;29(1):621-663.
11. Fahey LM, Wilson EB, Elsaesser H, Fistonich CD, McGavern DB, Brooks DG. Viral persistence redirects CD4 T cell differentiation toward T follicular helper cells. *J Exp Med*. 2011;208(5):987-999.
12. Glatman Zaretsky A, Taylor JJ, King IL, Marshall FA, Mohrs M, Pearce EJ. T follicular helper cells differentiate from Th2 cells in response to helminth antigens. *J Exp Med*. 2009;206(5):991-999.
13. Amé-Thomas P, Hoeller S, Artchounin C, et al. CD10 delineates a subset of human IL-4 producing follicular helper T cells involved in the survival of follicular lymphoma B cells. *Blood*. 2015;125(15):2381-2385.
14. Cannons JL, Lu KT, Schwartzberg PL. T follicular helper cell diversity and plasticity. *Trends Immunol*. 2013;34(5):200-207.
15. Vinuesa CG, Tangye SG, Moser B, Mackay CR. Follicular B helper T cells in antibody responses and autoimmunity. *Nat Rev Immunol*. 2005;5(11):853-865.
16. Chung Y, Tanaka S, Chu F, et al. Follicular regulatory T cells expressing Foxp3 and Bcl-6 suppress germinal center reactions. *Nat Med*. 2011;17(8):983-988.
17. Linterman MA, Pierson W, Lee SK, et al. Foxp3+ follicular regulatory T cells control the germinal center response. *Nat Med*. 2011;17(8):975-982.
18. Chang PP, Barral P, Fitch J, et al. Identification of Bcl-6-dependent follicular helper NKT cells that provide cognate help for B cell responses. *Nat Immunol*. 2011;13(1):35-43.
19. King IL, Fortier A, Tighe M, et al. Invariant natural killer T cells direct B cell responses to cognate lipid antigen in an IL-21-dependent manner. *Nat Immunol*. 2011;13(1):44-50.

20. Caccamo N, Battistini L, Bonneville M, et al. CXCR5 identifies a subset of Vgamma9Vdelta2 T cells which secrete IL-4 and IL-10 and help B cells for antibody production. *J Immunol*. 2006;177(8):5290-5295.

21. Harty JT, Tvinnereim AR, White DW. CD8+ T cell effector mechanisms in resistance to infection. *Annu Rev Immunol*. 2000;18(1):275-308.

22. Jiang J, Champion CI, Wei B, Liu G, Kelly KA. CD8+CXCR5+ T cells regulate pathology in the genital tract. *Infect Dis Obstet Gynecol*. 2013;2013: 813238.

23. Kim HJ, Verbinnen B, Tang X, Lu L, Cantor H. Inhibition of follicular T-helper cells by CD8(+) regulatory T cells is essential for self tolerance. *Nature*. 2010; 467(7313):328-332.

24. Kiniwa Y, Miyahara Y, Wang HY, et al. CD8+ Foxp3+ regulatory T cells mediate immunosuppression in prostate cancer. *Clin Cancer Res*. 2007;13(23): 6947-6958.

25. Chaput N, Louafi S, Bardier A, et al. Identification of CD8+CD25+Foxp3+ suppressive T cells in colorectal cancer tissue. *Gut*. 2009;58(4):520-529.

26. Wei S, Kryczek I, Zou L, et al. Plasmacytoid dendritic cells induce CD8+ regulatory T cells in human ovarian carcinoma. *Cancer Res*. 2005;65(12): 5020-5026.

27. Im SJ, Hashimoto M, Gerner MY, et al. Defining CD8+ T cells that provide the proliferative burst after PD-1 therapy. *Nature*. 2016;537(7620):417-421.

28. Leong YA, Chen Y, Ong HS, et al. CXCR5(+) follicular cytotoxic T cells control viral infection in B cell follicles. *Nat Immunol*. 2016;17(10):1187-1196.

29. He R, Hou S, Liu C, et al. Follicular CXCR5-expressing CD8(+) T cells curtail chronic viral infection [published correction appears in Nature. 2016;540(7633):470]. *Nature*. 2016;537(7620):412-428.

30. Quigley MF, Gonzalez VD, Granath A, Andersson J, Sandberg JK. CXCR5+ CCR7- CD8 T cells are early effector memory cells that infiltrate tonsil B cell follicles. *Eur J Immunol*. 2007;37(12):3352-3362.

31. Xiao L, Jia L, Bai L, et al. Phenotypic and functional characteristics of IL-21-expressing CD8(+) T cells in human nasal polyps. *Sci Rep*. 2016;6(1):30362.

32. Perdomo-Celis F, Taborda NA, Rugeles MT. Follicular $CD8^+$ T cells: origin, function and importance during HIV infection. *Front Immunol*. 2017;8:1241.

33. Xing J, Zhang C, Yang X, et al. $CXCR5^+CD8^+$ T cells infiltrate the colorectal tumors and nearby lymph nodes, and are associated with enhanced IgG response in B cells. *Exp Cell Res*. 2017;356(1):57-63.

34. Swerdlow SH, Campo E, Harris NL, et al. WHO Classification of Tumours of Haematopoietic and Lymphoid Tissues. Lyon, France: IARC Press; 2008.

35. Misiak J, Tarte K, Amé-Thomas P. Flow cytometric detection and isolation of human tonsil or lymph node T follicular helper cells. *Methods Mol Biol*. 2015; 1291:163-173.

36. Duhen T, Pasero C, Mallet F, Barbarat B, Olive D, Costello RT. LIGHT costimulates CD40 triggering and induces immunoglobulin secretion; a novel key partner in T cell-dependent B cell terminal differentiation. *Eur J Immunol*. 2004;34(12):3534-3541.

37. Hutloff A, Dittrich AM, Beier KC, et al. ICOS is an inducible T-cell co-stimulator structurally and functionally related to CD28. *Nature*. 1999;397(6716): 263-266.

38. Choi YS, Kageyama R, Eto D, et al. ICOS receptor instructs T follicular helper cell versus effector cell differentiation via induction of the transcriptional repressor Bcl6. *Immunity*. 2011;34(6):932-946.

39. Gigoux M, Shang J, Pak Y, et al. Inducible costimulator promotes helper T-cell differentiation through phosphoinositide 3-kinase. *Proc Natl Acad Sci USA*. 2009;106(48):20371-20376.

40. Xu H, Li X, Liu D, et al. Follicular T-helper cell recruitment governed by bystander B cells and ICOS-driven motility. *Nature*. 2013;496(7446):523-527.

41. Rasheed AU, Rahn HP, Sallusto F, Lipp M, Müller G. Follicular B helper T cell activity is confined to CXCR5(hi)ICOS(hi) CD4 T cells and is independent of CD57 expression. *Eur J Immunol*. 2006;36(7):1892-1903.

42. Yang R, Masters AR, Fortner KA, et al. IL-6 promotes the differentiation of a subset of naive CD8+ T cells into IL-21-producing B helper CD8+ T cells. *J Exp Med*. 2016;213(11):2281-2291.

43. Pearce EL, Mullen AC, Martins GA, et al. Control of effector CD8+ T cell function by the transcription factor eomesodermin. *Science*. 2003;302(5647): 1041-1043.

44. Sanz I, Wei C, Lee FE, Anolik J. Phenotypic and functional heterogeneity of human memory B cells. *Semin Immunol*. 2008;20(1):67-82.

45. Hardtke S, Ohl L, Förster R. Balanced expression of CXCR5 and CCR7 on follicular T helper cells determines their transient positioning to lymph node follicles and is essential for efficient B-cell help. *Blood*. 2005;106(6):1924-1931.

46. Scheeren FA, Diehl SA, Smit LA, et al. IL-21 is expressed in Hodgkin lymphoma and activates STAT5: evidence that activated STAT5 is required for Hodgkin lymphomagenesis. *Blood*. 2008;111(9):4706-4715.

47. Kohrt H, Johannsen A, Hoppe R, et al. Dynamic CD8 T-cell responses to tumor-associated Epstein-Barr virus antigens in patients with Epstein-Barr virus-negative Hodgkin's disease. *Oncol Res*. 2009;18(5-6):287-292.

48. Nam-Cha SH, Montes-Moreno S, Salcedo MT, Sanjuan J, Garcia JF, Piris MA. Lymphocyte-rich classical Hodgkin's lymphoma: distinctive tumor and microenvironment markers. *Mod Pathol*. 2009;22(8):1006-1015.